Restoration of the $N = 82$ Shell Gap from Direct Mass Measurements of ^{132,134}Sn

M. Dworschak,[1,*] G. Audi,[2] K. Blaum,[1,3,4] P. Delahaye,[5] S. George,[1,3] U. Hager,[6] F. Herfurth,[1] A. Herlert,[5]
A. Kellerbauer,[4] H.-J. Kluge,[1,7] D. Lunney,[2] L. Schweikhard,[8] and C. Yazidjian[1]

[1]*GSI, Planckstraße 1, 64291 Darmstadt, Germany*
[2]*CSNSM-IN2P3-CNRS, Université de Paris Sud, 91405 Orsay, France*
[3]*Johannes Gutenberg-Universität, Institut für Physik, 55099 Mainz, Germany*
[4]*Max Planck Institute for Nuclear Physics, P.O. Box 103980, 69029 Heidelberg, Germany*
[5]*CERN, Physics Department, 1211 Geneva 23, Switzerland*
[6]*University of Jyväskylä, Department of Physics, P.O. Box 35 (YFL), 40014 Jyväskylä, Finland*
[7]*Ruprecht-Karls-Universität, Physikalisches Institut, 69120 Heidelberg, Germany*
[8]*Ernst-Moritz-Arndt-Universität, Institut für Physik, 17487 Greifswald, Germany*
(Received 11 November 2007; published 22 February 2008)

A high-precision direct Penning trap mass measurement has revealed a 0.5-MeV deviation of the binding energy of ^{134}Sn from the currently accepted value. The corrected mass assignment of this neutron-rich nuclide restores the neutron-shell gap at $N = 82$, previously considered to be a case of "shell quenching." In fact, the new shell gap value for the short-lived ^{132}Sn is larger than that of the doubly magic ^{48}Ca which is stable. The $N = 82$ shell gap has considerable impact on fission recycling during the r process. More generally, the new finding has important consequences for microscopic mean-field theories which systematically deviate from the measured binding energies of closed-shell nuclides.

Shell effects are fundamental pillars upholding nuclear structure. The so-called "magic" numbers indicate closed shells, corresponding to spherical nuclei that provide important benchmarks for theoretical descriptions. The advent of radioactive beams has brought to light surprising evidence that shell closures lose their magicity far from stability, in regions of extreme isospin imbalance. The term "shell quenching" [1] has been used in cases where the effect of a magic number is eroded to the point of disappearance, as in the case of $N = 20$ [2] and $N = 28$ [3]. The nuclear ground-state binding energy, through the mass, has been a traditional observable for shell effects [4]. While these effects are small, especially considering the much larger volume and surface contributions to the binding energy, they can now be probed by mass measurements using high-precision techniques over large areas of the nuclear chart [5,6].

The strength of the shell closures is important for nucleosynthesis via the rapid neutron capture process and consequently, masses have a considerable influence on the abundance distributions of heavy elements (see, for example, the work of Burbidge, Burbidge, Fowler, and Hoyle (BBFH) [7]). In their seminal work, BBFH elaborated the role of fission in the r process. This thread has been revived recently by Martínez-Pinedo *et al.* [8] who assert that the $N = 82$ shell gap plays a pivotal role in the neutron-consumption rate during the r process.

The strength of the ^{132}Sn shell, as derived from previous mass data, does not reflect a doubly magic nuclide whose vibrational (spherical) properties are well established from spectroscopy studies. One hypothesis, from β-spectroscopy studies, was that the $N = 82$ shell closure

might be quenched [9]. The present letter reports on the resolution of this conflict. It turns out that the strength of the ^{132}Sn shell closure was mistakenly determined to be too small. Our new, direct mass measurement of ^{134}Sn has revealed a 0.5-MeV discrepancy with respect to previous Q_β measurements [10,11]. This finally restores the shell closure to that expected for a doubly magic nuclide.

Mass measurements on the isotopes $^{127,131-134}$Sn were performed with the Penning trap mass spectrometer ISOLTRAP [12,13], installed at the online isotope separator ISOLDE [14] at CERN. The short-lived tin nuclides were produced by impinging 1.4-GeV proton beam pulses of up to 3×10^{13} protons every 1.2 s on a thick uranium-carbide target, heated to over 2000 °C. Since we expected a huge number of contaminant ions in the mass region of the isotopes of interest ($A \approx 130$, especially the Cs and Ba fission products), ^{34}S was injected as isotopically enriched vapor into the hot plasma ion source of ISOLDE. In this way, the Sn isotopes of interest formed molecular compounds, mass-shifted to the less contaminated region of heavier nuclides around $A \approx 164$, and we measured the masses of tin sulfides instead of the pure tin isotopes.

A yield of about 10^5 ions/s in the case of ^{134}Sn^{34}S$^+$ was observed. After ionization in a hot plasma ion source, the beam of nuclides was sent through a mass separator with a resolving power of about 3000 and was provided to ISOLTRAP at an energy of 60 keV.

At the ISOLTRAP mass spectrometer [12,13] a radio frequency quadrupole cooler and buncher is used to decelerate and accumulate the ions by collisional cooling in helium buffer gas [15]. They are accumulated in the potential minimum and finally extracted as a low-energy ion

bunch and injected into a preparation Penning trap. Here, a mass-selective buffer-gas cooling technique [16], with a resolving power $R = \nu/\Delta\nu$ of up to 10^5, is used to remove contaminant ions. The isobarically purified ion bunch is then transported to a precision Penning trap where the cyclotron frequency $\nu_c = qB/(2\pi m)$ is determined after some preparatory steps by the time-of-flight ion-cyclotron resonance (TOF-ICR) detection method [17,18]. q/m is the charge-to-mass ratio of the ion of interest stored in the field ($B = 5.9$ T) of a superconducting magnet.

An azimuthal RF field at the cyclotron frequency excites the ion motion in the precision trap. The resonance is detected by ejecting the trapped ions towards a channeltron detector [19] and measuring their time of flight. The time-of-flight resonance curve, as shown in Fig. 1 for ^{132}Sn^{34}S$^+$ and ^{134}Sn^{34}S$^+$, has its minimum at the cyclotron frequency, which is deduced by a fit of the theoretical line shape to the data points [18]. In the precision Penning trap a resolving power $R = \nu/\Delta\nu = 10^7$ and a relative uncertainty of down to 8×10^{-9} can be achieved [20] allowing to resolve even low-lying isomeric states [21,22].

The temperature-stabilized magnetic field is calibrated by determining the frequency of ^{133}Cs$^+$ which has a well-known mass [23]. For the reference measurements excitation times of $T_{RF} = 900$ ms and $T_{RF} = 1.2$ s were applied. The calibration, data analysis and uncertainty treatment were performed according to the procedure described in [20]. In addition to the uncertainty obtained by the fit curve a relative mass dependent error of $1.6 \times 10^{-10}/u(m - m_{ref})$ is added to correct for the uncertainty due to the mass difference of the ions of interest and the reference ions. Although we had shifted the mass range of our measurement from $A \approx 130$ to $A \approx 164$ by using molecular sidebands of SnS, we still observed a large number of contaminant molecular ions. A possible shift of the mea-
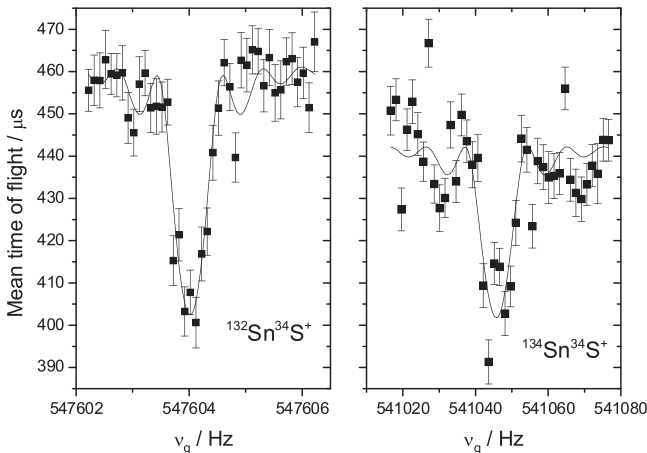
sured cyclotron frequency due to the presence of contaminations can be corrected by the so-called z-class analysis [20]. Here, the events per frequency step within one resonance curve are divided into three z classes according to the number of ions per cycle. For all classes the corresponding cyclotron frequency is determined. The cyclotron frequency is then extrapolated to the value for one ion per cycle. Contaminations have been identified and removed by mass-selective cleaning [22] for ^{130}Ba^{34}Cl$^+$, ^{167}Tm$^+$, ^{132}Ba^{35}Cl$^+$, ^{134}Ba^{34}S$^+$, ^{168}Yb$^+$ and ^{130}Ba^{35}Cl$^+$.

Resonance curves were measured for the nuclides $^{127,131-134}$Sn in molecular bond with ^{34}S. The frequency ratios and their uncertainties are given in Table I. In parallel to the Penning trap experiment the yields of all possible contaminations have been measured by γ-spectroscopy [24]. In a frequency window of ± 2 Hz corresponding to about ± 400 keV the yields of the most abundant contaminations were at least an order of magnitude less than the yields of the SnS isotopes of interest. Thus, we conclude that the z-class analysis copes very well with a potentially still remaining contamination.

The deduced mass excess values (D) of the investigated nuclides are listed in Table II. Figure 2 shows a comparison between the mass values obtained with ISOLTRAP and the literature values.

For the nuclide ^{127}Sn two resonance curves were taken with a cyclotron excitation time of $T_{RF} = 900$ ms. ^{127}Sn has an isomeric state at 4.7 keV [23] which could not be resolved. The ground-state mass excess was determined as $-83\,463(11)$ keV assuming an unknown production ratio of the two isomeric states. The new value is in agreement with the literature value of $-83\,499(25)$ keV, based on a Q_β measurement [25].

The half-life of the ground state of ^{131}Sn ($T_{1/2} = 56$ s) is approximately the same as that of the isomeric state ($T_{1/2} = 58.4$ s) whose excitation energy has been determined by Fogelberg *et al.* to be 65.1 keV [26]. Even with an excitation time of 9 s, these states could not be resolved due to damping of the ion motion in the precision trap. The ratio of the production rates of the two states is roughly known (^{131m}Sn/$^{131g+m}$Sn $= 0.65(15)$, based on [27,28]). Therefore, the measured cyclotron frequency is treated as a weighted average of both nuclear states [23].

FIG. 1. Cyclotron resonances of ^{132}Sn^{34}S$^+$ with an excitation time of 1.5 s and ^{134}Sn^{34}S$^+$ with an excitation time of 100 ms. The solid line is a fit of the expected line shape to the data points [18].

TABLE I. Frequency ratios $r = \frac{\nu_{c,ref}}{\nu_c}$ of the measured nuclides. ^{133}Cs$^+$ from an offline ion source with $m(^{133}$Cs$) = 132.905\,451\,933(24)$ u [23] was used as the reference ion.

Ion	$r = \nu_{c,ref}/\nu_c$
^{127}Sn^{34}S$^+$	1.210 472 415 5(874)
^{131}Sn^{34}S$^+$	1.240 619 521 0(268)
^{132}Sn^{34}S$^+$	1.248 149 146 5(577)
^{133}Sn^{34}S$^+$	1.255 719 368(187)
^{134}Sn^{34}S$^+$	1.263 280 08(122)

TABLE II. Half-life $T_{1/2}$ [23], mass excess $D_{ISOLTRAP}$ obtained by the present experiment, mass excess D_{AME} of AME2003 [23], and the differences $\Delta D = D_{AME} - D_{ISOLTRAP}$ of the measured nuclides.

Nuclide	$T_{1/2}$	$D_{ISOLTRAP}$ (keV)	D_{AME} (keV)	ΔD (keV)
^{127}Sn	2.10 h	$-83\,463(11)$	$-83\,499(25)$	-36
^{131}Sn	56.0 s	$-77\,264(10)$	$-77\,314(21)$	-50
^{132}Sn	39.7 s	$-76\,547(7)$	$-76\,554(14)$	-7
^{133}Sn	1.45 s	$-70\,847(23)$	$-70\,950(40)$	-103
^{134}Sn	1.12 s	$-66\,320(150)$	$-66\,800(100)$	-480

The result of the present ^{132}Sn measurement agrees with the atomic-mass evaluation (AME) value of 2003, which was mainly (64%) derived from a former ISOLTRAP measurement [29]. The mass of this nuclide could be determined with an uncertainty of only $\delta m = 7$ keV, which represents a twofold improvement in accuracy as compared to the earlier measurement. A cyclotron resonance curve of this nuclide is shown in Fig. 1 (left).

For the nuclides ^{133}Sn and ^{134}Sn the measurements presented here are the first direct mass measurements with a Penning trap. With four resonance curves taken for ^{133}Sn^{34}S$^+$ the mass excess was determined to be $-70\,847(23)$ keV. This value deviates by 103 keV from the literature value derived from two Q_β measurements [10,30].

Because of lack of beam time only one resonance curve of ^{134}Sn^{34}S$^+$ could be recorded (see Fig. 1, right). Using $T_{RF} = 100$ ms, an uncertainty in the mass excess of $\delta D = 150$ keV was obtained, which is dominated by the limited statistics. Our value for the mass excess disagrees with the literature value from Q_β measurements [10] by 480 keV.

This deviation may be due to some high-lying decay branch that could have been missed in the β-decay measurement.

The new mass excess values reported in this work have important consequences for nuclear structure. The two-neutron separation energy $S_{2n} = B(N, Z) - B(N - 2, Z)$ (where B is the binding energy) decreases steadily with increasing neutron number N. A sudden drop in S_{2n} is observed for magic neutron numbers N_0, for which the neutron-shell gap is defined by

$$\Delta_n(N_0, Z) = S_{2n}(N_0, Z) - S_{2n}(N_0 + 2, Z). \quad (1)$$

This quantity is shown in Fig. 3 (top) for the magic neutron numbers $N_0 = 20, 28, 50, 82$, and 126, as a function of proton number Z (note the log scale). The highest shell gaps (over 8 MeV) correspond to the $N = Z$ nuclides ^{40}Ca and ^{56}Ni, which have additional binding energy due to the so-called Wigner effect (see discussion in [4]). The average gap is around 5 MeV with local maxima corresponding to doubly magic nuclides (the so-called mutually-enhanced magicity, first discussed in [31]). For lower Z, i.e., more exotic species, the $N_0 = 20$ shell is seen to be quenched. Figure 3 (bottom) shows the case for $N_0 = 82$, where the AME2003 [23] maximum did not occur at ^{132}Sn but one proton higher. The new mass value of ^{134}Sn changes the $N_0 = 82$ neutron-shell gap significantly (see unfilled square in Fig. 3). The old peak at $Z = 51$ has now been eliminated.
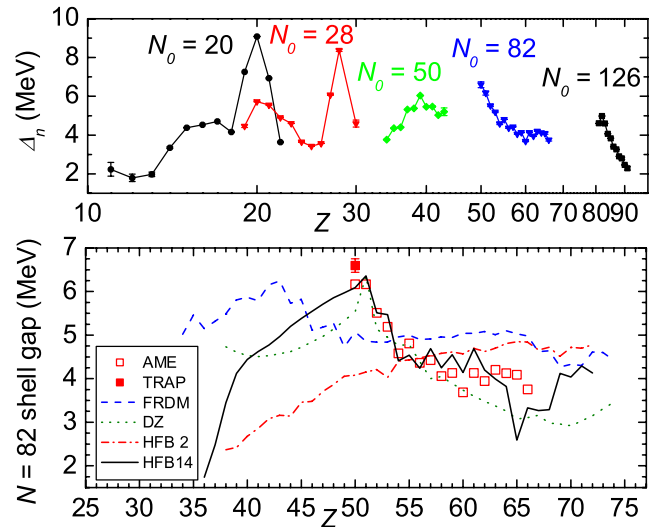
FIG. 3 (color online). Experimental neutron-shell gaps as a function of Z for magic neutron numbers $20 \leq N_0 \leq 126$ (top) and for $N_0 = 82$ (bottom) in comparison to the theoretical models FRDM [39], Duflo-Zuker (DZ) [40], HFB-2 [41] and HFB-14 [32]. The new ISOLTRAP value (filled square) shows that the shell gap is now maximum for the magic proton number $Z = 50$. The other experimental data (open squares) are taken from [23]. In the upper part of the figure only the new ISOLTRAP value is plotted at $N_0 = 82$ and $Z = 50$.
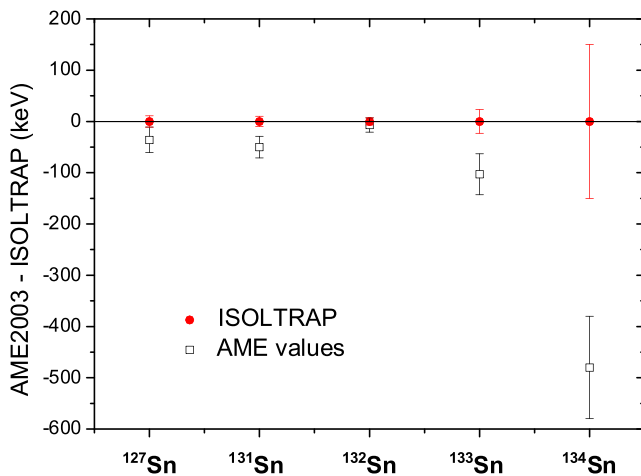

FIG. 2 (color online). Comparison of the results of the ISOLTRAP mass measurements with the literature values taken from the AME2003 database [23]. The ISOLTRAP data define the zero line.

Questions related to r process nucleosynthesis depend very strongly on mass models. Figure 3 (bottom) also shows some predicted $N = 82$ shell gap values. A similar figure was published in [4] along with detailed descriptions of the corresponding mass models. It is striking that all three models describe the shell gap differently. The Duflo-Zuker model follows the experimental data very well, although they find a maximum at $Z = 51$, whereas the FRDM does not. Also shown in Fig. 3 are two Hartree-Fock-Bogoliubov (HFB) microscopic mass models. The older HFB-2, originally shown in [4] has evolved considerably with the latest version HFB-14 [32] showing an excellent prediction of the shell gap. Like DZ, HFB-14 shows a maximum at $Z = 51$, rather than $Z = 50$, but only due to spurious effects contributing an uncertainty of roughly 0.2 MeV to the calculation [33]. The HFB evolution can be seen in their suite of papers [32,34] where an important role is played by pairing, the energy contribution of which emulates the binding brought by correlations beyond the mean field. Such correlations are treated by Bender *et al.* [35,36], who constructed a mass table for even-even nuclides taking quadrupole correlations into account. Note that their force (a Skyrme force, like that of HFB-14) is only adjusted to the properties of doubly magic nuclides and as such *overbinds* such nuclides, contrary to the case of the HFB mass models.

An important distinction must be made between a local maximum (mutually-enhanced magicity) and quenching. While we cannot predict if and where quenching will occur, we have refuted the one piece of evidence that was compatible with quenching of the $N = 82$ shell and therefore contradicts arguments previously put forth for modifying the r process abundances [37]. This stronger shell gap is interesting in light of a recent hypothesis by Martínez-Pinedo *et al.* [8] concerning fission in the r process. The conclusion of their work is that "...mass models with strong shell gaps yield final abundances that are practically independent of the conditions once the neutron-to-seed ratio is large enough." A strong shell gap slows down the r process and creates more neutrons (by photodisintegration), causing more fission. Though uncertainties persist, this conclusion could be supported by the recent metal-poor star observations that seem to show universal abundance patterns of heavy elements [38]. Thus, the tendency of shell quenching in the r process merits reconsideration.

*Corresponding author.
m.dworschak@gsi.de

[1] J. Dobaczewski *et al.*, Nucl. Phys. A **422**, 103 (1984).
[2] C. Thibault *et al.*, Phys. Rev. C **12**, 644 (1975).
[3] F. Sarazin *et al.*, Phys. Rev. Lett. **84**, 5062 (2000).
[4] D. Lunney *et al.*, Rev. Mod. Phys. **75**, 1021 (2003).
[5] K. Blaum, Phys. Rep. **425**, 1 (2006).
[6] Special issue on Ultra-Accurate Mass Spectrometry and Related Topics, edited by L. Schweikhard and G. Bollen [Int. J. Mass Spectrom. **251**, 85 (2006)].
[7] E. M. Burbidge, G. R. Burbidge, W. A. Fowler, and F. Hoyle, Rev. Mod. Phys. **29**, 547 (1957).
[8] G. Martínez-Pinedo *et al.*, Proc. Sci. NIC-IX (2006) 064.
[9] I. Dillmann *et al.*, Phys. Rev. Lett. **91**, 162503 (2003).
[10] K. A. Mezilev *et al.*, Phys. Scr. **T56**, 272 (1995).
[11] B. Fogelberg *et al.*, Phys. Rev. Lett. **82**, 1823 (1999).
[12] G. Bollen *et al.*, Nucl. Instrum. Methods Phys. Res., Sect. A **368** 675 (1996).
[13] F. Herfurth *et al.*, J. Phys. B **36**, 931 (2003).
[14] E. Kugler, Hyperfine Interact. **129**, 23 (2000).
[15] F. Herfurth *et al.*, Nucl. Instrum. Methods Phys. Res., Sect. A **469**, 254 (2001).
[16] G. Savard *et al.*, Phys. Lett. A **158**, 247 (1991).
[17] K. Blaum *et al.*, J. Phys. B **36**, 921 (2003).
[18] M. König *et al.*, Int. J. Mass Spectrom. Ion Processes **142**, 95 (1995).
[19] C. Yazidjian *et al.*, Hyperfine Interact. **173**, 181 (2006).
[20] A. Kellerbauer *et al.*, Eur. Phys. J. D **22**, 53 (2003).
[21] J. Van Roosbroeck *et al.*, Phys. Rev. Lett. **92**, 112501 (2004).
[22] K. Blaum *et al.*, Europhys. Lett. **67**, 586 (2004).
[23] G. Audi *et al.*, Nucl. Phys. **A729**, 337 (2003).
[24] U. Köster *et al.*, Nucl. Instrum. Methods Phys. Res., Sect. A (to be published).
[25] E. Lund *et al.*, Nucl. Phys. A **286**, 403 (1977).
[26] B. Fogelberg *et al.*, Phys. Rev. C **70**, 034312 (2004).
[27] C. Stone, Ph.D. thesis, University of Maryland, 1987.
[28] H. Gausemel *et al.* (to be published).
[29] G. Sikler *et al.*, Nucl. Phys. **A763**, 45 (2005).
[30] J. Blomquist *et al.*, Z. Phys. A **314**, 199 (1983).
[31] N. Zeldes *et al.*, Nucl. Phys. **A399**, 11 (1983).
[32] S. Goriely, M. Samyn, and J. M. Pearson, Phys. Rev. C **75**, 064312 (2007).
[33] S. Goriely and J. M. Pearson (private communication).
[34] J. M. Pearson and S. Goriely, Nucl. Phys. **A777**, 623 (2006).
[35] M. Bender *et al.*, Phys. Rev. Lett. **94**, 102503 (2005).
[36] M. Bender *et al.*, Phys. Rev. C **73**, 034322 (2006).
[37] B. Pfeiffer *et al.*, Z. Phys. A **357**, 235 (1997).
[38] J. J. Cowan and C. Sneden, Nature (London) **440**, 1151 (2006).
[39] P. Møller *et al.*, At. Data Nucl. Data Tables **59**, 185 (1995).
[40] J. Duflo and A. P. Zuker, Phys. Rev. C **52**, R23 (1995).
[41] S. Goriely *et al.*, Phys. Rev. C **66**, 024326 (2002).